

A Highly Efficient 1.95-GHz, 18-W Asymmetric Multilevel Outphasing Transmitter for Wideband Applications

Philip A. Godoy, SungWon Chung, Taylor W. Barton, David J. Perreault, and Joel L. Dawson
Microsystems Technology Laboratories, Massachusetts Institute of Technology, Cambridge, MA 02139, USA

Abstract—A 1.95-GHz asymmetric multilevel outphasing (AMO) transmitter with class-E GaN power amplifiers (PAs) and discrete supply modulators is presented. AMO transmitters achieve improved efficiency over envelope tracking (ET) transmitters by replacing the continuous supply modulator with a discrete supply modulator implemented with a fast digital switching network. Outphasing modulation is used to provide the required fine output envelope control. A 4-level supply modulator is implemented that allows for fast and efficient discrete envelope modulation with up to 28-V supply voltages using low-voltage gate drivers and time-alignment logic. With two class-E GaN PAs that achieve 62.5% power-added efficiency (PAE) at 40-dBm peak output power, the AMO transmitter delivers 42.6-dBm peak output power at 1.95-GHz. For a 16-QAM signal at 36-dBm output power, the transmitter achieves 44.2/42.8/41.4% average system efficiency and 2.0/2.1/3.1% EVM for 10/20/40-MHz channel bandwidth, respectively.

Index Terms—power amplifier, base station, outphasing, LINC, discrete supply modulator, digital predistortion

I. INTRODUCTION

Achieving high efficiency for wideband, high peak-to-average power ratio (PAPR) signals is one of the most difficult problems for modern wireless transmitters. As one of the most promising high-efficiency PAs, an envelope tracking (ET) PA [1], [2] has been demonstrated with excellent efficiency with 3.84-MHz bandwidth WCDMA signals. ET PAs use a switching power converter to continuously modulate the supply of a PA to improve efficiency at significant power backoff. The tradeoff that these systems face is ultimately between modulation bandwidth and efficiency in the power converter; in general, the higher the modulation bandwidth, the lower the efficiency. By including a feedforward path in the supply modulator, a continuous supply modulator for ET PAs was demonstrated to modulate 10-MHz signals with more than 50% PAE [1]. As the bandwidth increases, however, it becomes increasingly difficult for the supply modulator to maintain high efficiency with high power handling capability.

Fig. 1 shows the asymmetric multilevel outphasing (AMO) architecture with discrete supply modulator [3], [4], which has the potential to allow even larger baseband bandwidths while maintaining high average efficiency and high linearity. The supply modulator for AMO transmitters only provides a discrete set of envelope amplitudes for the PAs. Fine envelope amplitude modulation is achieved by outphasing modulation. Unlike ET PAs, the discrete supply modulator can operate open-loop without feedback or oversampling. Thus, high-efficiency and wide-bandwidth supply modulation are allowed. In this paper, we demonstrate the highest-efficiency AMO implementation reported in the literature.

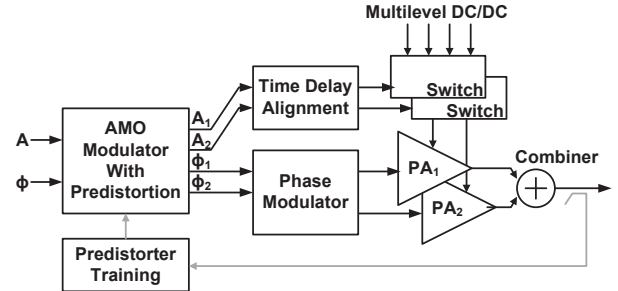


Fig. 1. Asymmetric multilevel outphasing (AMO) architecture with discrete supply modulator.

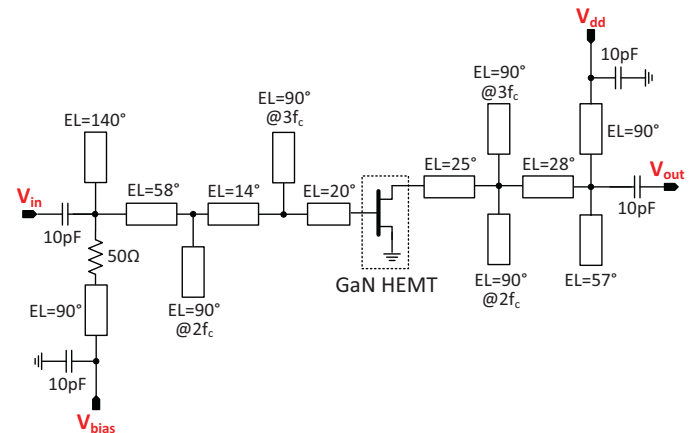


Fig. 2. Circuit schematic of the 10-W 1.95-GHz class-E GaN PA.

II. CLASS-E GAN POWER AMPLIFIER

Fig. 2 shows the circuit schematic of the 10-W 1.95-GHz class-E GaN PA designed for the AMO transmitter prototype. The PA was designed using the methodology described in [5]. The harmonic terminations were implemented using quarter-wave open-circuit stubs. Load-pull and source-pull simulations were performed in the Agilent advanced design simulator (ADS) to characterize the optimum output and input impedances for the Cree GaN CGH40010 transistor. The maximum PAE from simulation, including losses from printed circuit board (PCB) traces and discrete components, was 80.1% with 39.4-dBm output power and 12.8-dB gain at V_{DD} of 28 V. Fig. 3 shows the drain voltage and current waveforms after deembedding package parasitics, exhibiting the zero-voltage switching characteristics of class-E operation.

Fig. 4 shows the fabricated class-E GaN HEMT PA, made with a low-loss Rogers 4350B dielectric. The PA was designed

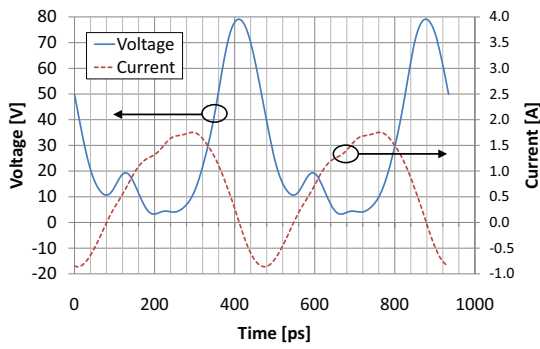


Fig. 3. Simulated drain voltage and current for the class-E GaN PA after deembedding package parasitics, indicating class-E operation. The design frequency was 2.14 GHz.

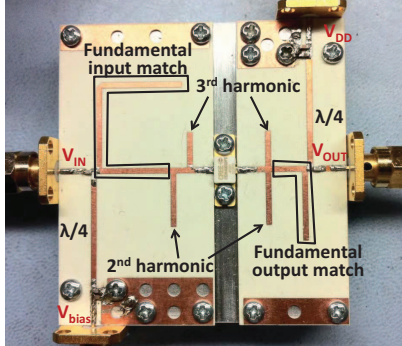


Fig. 4. Photograph of the fabricated class-E GaN PA.

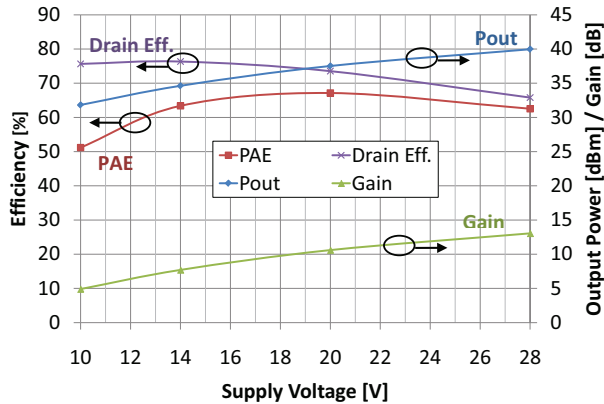


Fig. 5. Measured PAE, drain efficiency, output power, and gain of the class-E GaN PA at 1.95 GHz.

for a target operating frequency of 2.14 GHz, but after fabrication the optimum frequency was found to be 1.95 GHz. Fig. 5 shows the measured PAE, drain efficiency, output power, and gain of the implemented Class-E GaN PA at 1.95 GHz. At the 40-dBm peak output power, the PAE is 62.5% with 13-dB gain. The peak PAE is 67% with 20-V supply voltage. Although drain efficiency is better at lower supply voltage, the PAE is degraded due to the fixed input power used to drive the PA. The PA operating frequency was chosen for maximum peak output power.

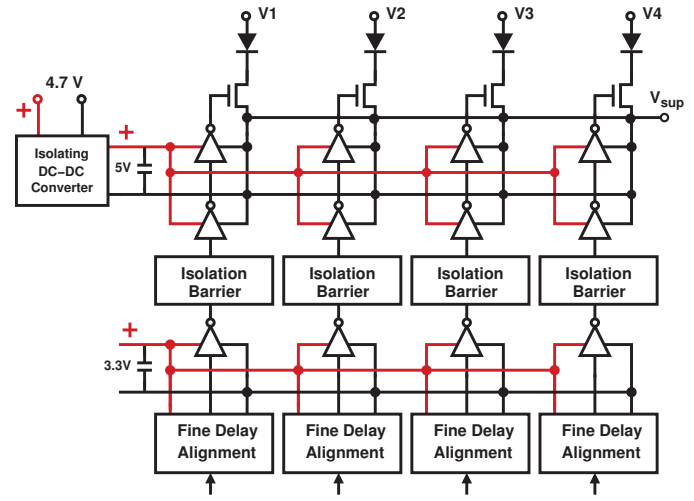


Fig. 6. 4-level discrete supply modulator.

III. DISCRETE SUPPLY MODULATOR

Fig. 6 shows the circuit schematic of the 4-level discrete supply modulator implemented in this work. Silicon LDMOS transistors from Polyfet (L8821P) were used for the supply voltage switches, and reverse current flow was prevented by using SS16 Schottky diodes from Fairchild Semiconductor. The gates of the power supply switches are driven with NC7WZ04 inverters from Fairchild Semiconductor. A 1-W isolated, unregulated dc-dc converter (TI model DCP010505BP) provides the 5-V power supply for the inverters driving the supply switch gates, whose reference ground potential is determined by the supply modulator amplitude setting. This low-voltage configuration reduces the power loss associated with driving the gates of the power supply switches, which must block voltages up to 28 V. Another source of power loss in the discrete supply modulator is due to the diode voltage drop, which is acceptable in base-station applications where the supply voltages are as high as 28 V. The inverter gate drivers are driven by Si8423 digital isolators from Silicon Labs, which are in turn driven by MC100EP196B programmable delay chips from ON-Semiconductor. The delay chips implement fine delay adjustment for time alignment between the supply switch control signals as well as time alignment between the amplitude and phase paths.

Fig. 7 shows the measured step response of the AMO transmitter output envelope when the supply voltage is changed from 7.5 V to 13 V for both PAs. The envelope settles in less than 15 ns. The nonzero settling time is caused by the parasitic inductances and capacitances of the discrete components and the PCB traces. Although nonzero settling time of the supply modulator introduces error-vector magnitude (EVM) and spectrum degradation, 30–40-dBc adjacent channel power ratio (ACPR) with up to 40-MHz channel bandwidth can be obtained without any step response calibration or correction. Because the phase modulator typically provides much faster settling time, when higher ACPR is desired, a phase-domain

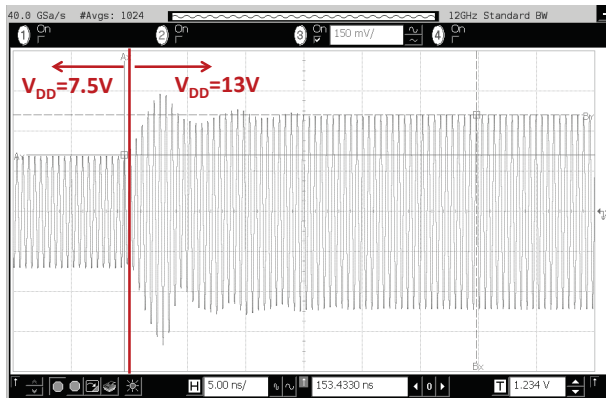


Fig. 7. Measured step response of the transmitter output envelope when the supply voltage is changed from 7.5 V to 13 V.

envelope-correction technique could be implemented.

IV. TRANSMITTER MEASUREMENT RESULTS

Fig. 8 shows the prototype 18-W, 1.95-GHz AMO transmitter, which uses two class-E GaN PAs and two discrete supply modulators. Digitally pre-distorted baseband data was generated by MATLAB after characterizing the AMO transmitter with a narrowband training signal. The two phase modulators were each implemented by a 16-bit dual-channel DAC evaluation board from Analog Devices (AD9779A). An FPGA provides the digital inputs to the phase modulators and the discrete supply modulators, and also performs coarse time alignment between the phase and amplitude paths. Fine time alignment is performed by programmable delay lines in each supply modulator. The supply modulators provide two independent supply voltages selected from four different power supplies to the two class-E PAs.

Fig. 9 shows the measured AMO transmitter total efficiency vs. output power as the supply voltage to both PAs is varied. Here we define the total efficiency as $\eta_{tot} = P_{out}/(P_{DC} + P_{in})$. It should be noted that the efficiency numbers include the insertion loss from the isolating power combiner, which is approximately 0.4 dB. For a given number of supply voltage levels, this data can be used to find the optimum supply voltages that maximize the efficiency for a given probability density function (PDF) [3]. In this work, we test the system with a 16-QAM signal with a PAPR of 6.5 dB, the PDF of which is shown in Fig. 9. The corresponding optimum efficiency curves for both 2 and 4 available supply voltages are also shown in the figure.

Fig. 10 shows the measured static nonlinearity of the AMO transmitter output amplitude and phase depending on the supply voltage combination and the outphasing angle. There are 7 different curves, each for a different combination of supply voltages for the two outphased PAs. A lookup table (LUT) constructed from the data in Fig. 10 implements the digital predistortion (DPD) to correct the static nonlinearity.

Fig. 11 shows the average system efficiency, ACPR, and EVM of the prototype AMO transmitter for the 16-QAM signal

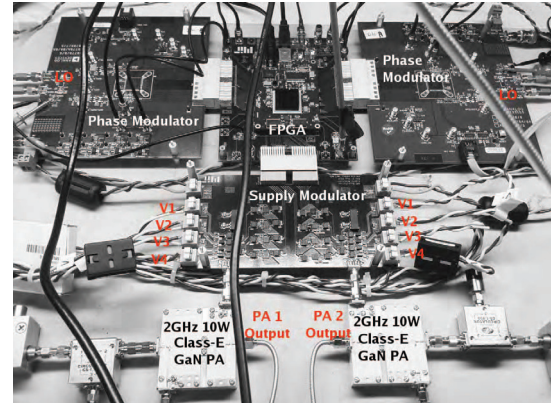
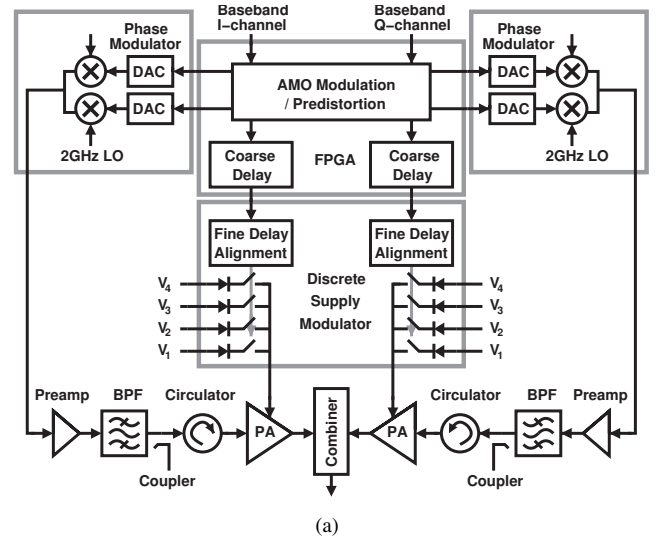


Fig. 8. Prototype implementation of the 18-W 1.95-GHz AMO transmitter with discrete supply modulators and class-E GaN PAs. (a) block diagram, (b) photograph.

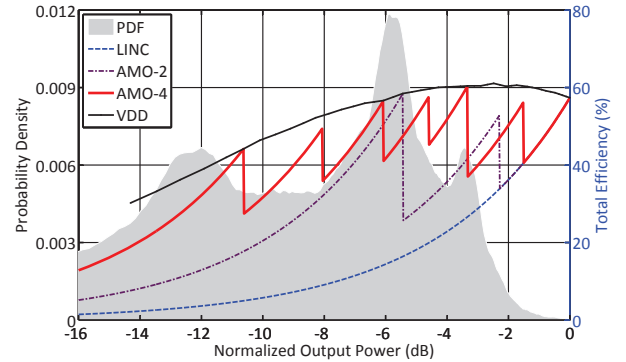


Fig. 9. Measured efficiency vs. output power for the AMO prototype, along with the optimized amplitude levels for a 16-QAM signal with 6.5-dB PAPR. The PDF of the 16-QAM signal is also shown.

transmission with various channel bandwidths from 2.5 to 40 MHz. For comparison purposes, we also show the results for the LINC (linear amplification of nonlinear components) case, when only a single supply voltage is used for both PAs. The

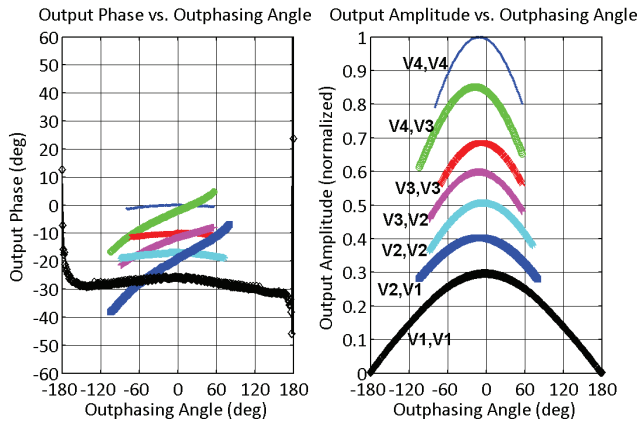


Fig. 10. Measured static nonlinearity of the AMO transmitter output amplitude and phase. Each curve corresponds to a different combination of supply voltages for the two outphased PAs.

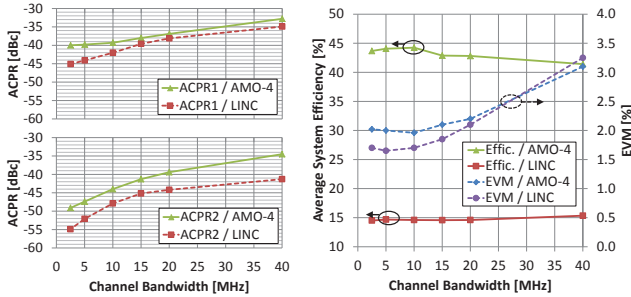


Fig. 11. Performance comparison for LINC and 4-level AMO with 6.5-dB PAPR 16-QAM transmission for various channel bandwidths.

sampling rate of the digital data was set to 10x the symbol rate for all channel bandwidths except for 40 MHz, in which case the sampling rate was 200MHz (5x the symbol rate). This is due to the speed limitation of the DACs used in the phase modulators. The average system efficiency numbers include the dynamic power consumption from the discrete supply modulators and is defined as $\eta_{sys} = P_{out}/(P_{DC} + P_{in} + P_{SupMod})$. From the plots, we can see a significant improvement in the efficiency for 4-level AMO vs. LINC. However, the ACPR and EVM are degraded because of the occurrence of glitches in the output envelope due to the finite settling time of the discrete supply modulators. It should be noted that the efficiency of the AMO transmission only begins to slowly degrade when the signal bandwidth exceeds 10 MHz. This demonstrates the relatively high efficiency of the discrete supply modulators compared to continuous supply modulators for wideband signal transmission.

Fig. 12 and Fig. 13 show the spectrum of the 16-QAM signal transmission at 2.5-MSym/s and 40-MSym/s, respectively. The curves labeled “DAC” show the spectrum using just the phase modulators without the PAs. At 20-MHz, 37-dB ACPR1 and 2.2% EVM is achieved with 42.8% average system efficiency. The LINC transmission at the same symbol rate achieves 38-dB ACPR1, 2.1% EVM, and 14.6% efficiency. The efficiency improvement with 4-level AMO vs. LINC is almost 3x.

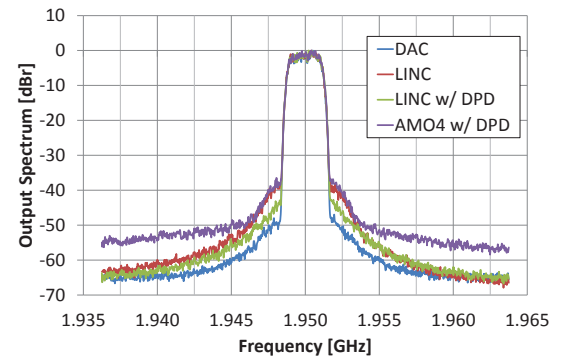


Fig. 12. Transmit spectrum for the 2.5-MHz bandwidth 16-QAM signal.

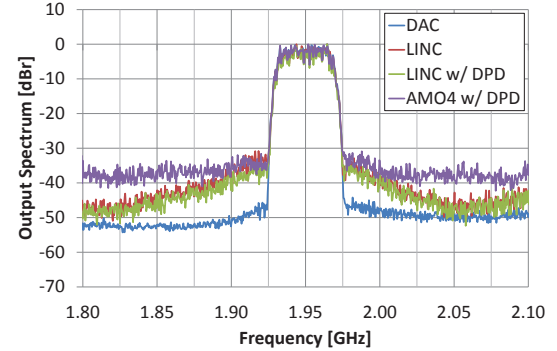


Fig. 13. Transmit spectrum for the 40-MHz bandwidth 16-QAM signal.

V. CONCLUSION

We demonstrate a 1.95-GHz asymmetric multilevel outphasing (AMO) transmitter for 3G/4G base-station applications. With two Class-E GaN PAs that achieve 62.5% PAE at 40-dBm peak output power, the AMO transmitter delivers 42.6-dBm peak output power at 1.95 GHz. For a 16-QAM signal at 36-dBm output power, the transmitter achieves 44.2/42.8/41.4% average system efficiency and 2.0/2.1/3.1% EVM for 10/20/40-MHz channel bandwidth, respectively. The results illustrate the potential of the AMO architecture for both high-efficiency and wide-bandwidth power amplification.

REFERENCES

- [1] C. Hsia *et al.*, “Wideband high efficiency digitally-assisted envelope tracking power amplifiers,” in *IEEE MTT-S Int’l Microwave Symp. Dig.*, May 2010, pp. 672–675.
- [2] J. Moon *et al.*, “Doherty amplifier with envelope tracking for high efficiency,” in *IEEE MTT-S Int’l Microwave Symp. Dig.*, May 2010, pp. 1086–1089.
- [3] S. Chung *et al.*, “Asymmetric multilevel outphasing architecture for multi-standard transmitters,” in *IEEE Radio Freq. Int. Circ. Symp. Dig. Tech. Papers*, June 2009.
- [4] J. Hur *et al.*, “Highly efficient uneven multi-level LINC transmitter,” *Electronics Lett.*, vol. 45, no. 16, pp. 837–838, July 2009.
- [5] D. T.-T. Wu *et al.*, “First-pass design of high efficiency power amplifiers using accurate large signal models,” in *IEEE Wireless and Microwave Tech. Conf.*, 2010, pp. 1–4.